lulinのtTJ局在を規定する因子としてangulin familyが同定され，ようやくtTJ構成タンパク質も詳らかにされつつあり[30)~32)]，bTJ制御とtTJ制御による吸収促進特性の相違（組織特異性，透過物質選択性），bTJ制御とtTJ制御のコンビネーションによる吸収促進効果の解析などを通じて，近い将来第三世代のTJ modulatorが誕生すると期待される。また，CLを介した細胞間隙輸送経路とトランスポーターを介した細胞内輸送経路がカップリングしていることも示されており，新しい吸収促進戦略の確立が期待される[33)]。

半世紀以上前にEDTAによって始まった上皮バリア制御による吸収促進研究は，TJシールの分子基盤の解明と相俟ってCLを標的としたターゲットベースの粘膜吸収促進戦略へと発展を遂げ，さらに最近tTJ構成タンパク質を標的とした吸収促進法の萌芽も生まれつつある。しかしながら，依然としてTJを標的とした吸収促進はC-CPEを用いてPOCが確立されているにすぎず，C-CPEに代わるペプチドおよびケミカルタイプのdruggable CL binderの開発は進んでいない。これは，CLタンパク質精製系が確立されていないこと（CL-4のみ確立），CLの立体構造が解析されていないことに起因しており，これらの課題克服に向けて国内外においてチャレンジが続いている。

本稿で紹介したbTJおよびtTJの分子基盤は，京都大学月田承一郎先生のグループ，神戸大学古瀬幹夫先生のグループ，大阪大学月田早智子先生のグループによってなされてきたものであり，近い将来，再び日本において新たなブレークスルーが引き起こされ，日本発の吸収促進剤が開発されることを願い，本稿の結びとしたい。

【謝　辞】

本稿を執筆する機会を与えていただいた大阪大学大学院薬学研究科中川晋作先生をはじめとした関係者の皆様方に衷心よりお礼申し上げます。また，本稿で紹介したデータは昭和薬科大学薬剤学教室，大阪大学大学院薬学研究科生体機能分子化学分野において実施されたものであり，相互作用を頂戴したすべての方々に敬意を表すると同時に心よりお礼申し上げます。なお，本稿で紹介しているデータの一部は，文部科学省科学研究費補助金（課題番号：21689006，24390042），厚生労働科学研究費補助金のサポートにより実施されたものである。

【引用・参考文献】

1) E. Windsor, G. E. Cronheim：*Nature*, **190**, 263 (1961).
2) S. Tsukita, et al.：*Oncogene*, **27**, 6930 (2008).
3) M. G. Farquhar, G. E. Palade：*J. Cell Biol.*, **17**, 375 (1963).
4) A. W. Sedar, J. G. Forte：*J. Cell Biol.*, **22**, 173 (1964).
5) B. J. Aungst：*J. Pharm. Sci.*, **89**, 429 (2000).
6) B. Kachar, T. S. Reese：*Nature*, **296**, 464 (1982).
7) P. Pinto da Silva, B. Kachar：*Cell*, **28**, 441 (1982).
8) E. S. Swenson, et al.：*Pharm. Res.*, **11**, 1501 (1994).
9) E. S. Swenson, et al.：*Pharm. Res.*, **11**, 1132 (1994).
10) M. Furuse, et al.：*J. Cell Biol.*, **123**, 1777 (1993).
11) V. Wong, B. Gumbinder：*J. Cell Biol.*, **136**, 399 (1997).
12) M. Furuse, et al.：*J. Cell Biol.*, **141**, 1539 (1998).
13) M. Saitou, et al.：*J. Cell Biol.*, **141**, 397 (1998).
14) M. Furuse：*Biochim. Biophys. Acta*, **1788**, 813 (2009).
15) M. Furuse, S. Tsukita：*Trends Cell Biol.*, **16**, 181 (2006).
16) N. Sonoda, et al.：*J. Cell Biol.*, **147**, 195 (1999).
17) K. Mineta, et al.：*FEBS Lett.*, **585**, 606 (2011).
18) M. Kondoh, et al.：*Drug Discov. Today*, **13**, 180 (2008).
19) J. Katahira, et al.：*J. Cell Biol.*, **136**, 1239 (1997).
20) B. A. McClane, G. Chakrabarti：*Anaerobe*, **10**, 107 (2004).
21) B. A. McClane：*J. Food Saf.*, **12**, 237 (1992).
22) M. Kondoh, et al.：*Mol. Pharmacol.*, **67**, 749 (2005).
23) H. Uchida, et al.：*Biochem. Pharmacol.*, **79**, 1437 (2010).
24) A. Takahashi, et al.：*J. Control. Release*, **108**, 56 (2005).
25) A. Takahashi, et al.：*Biochem. Pharmacol.*, **75**, 1639 (2008).
26) H. Kakutani, et al.：*PLoS One*, **6**, e16611 (2011).
27) T. Sakihama, et al.：*J. Biotechnol.*, **135**, 28 (2008).
28) A. Takahashi, et al.：*Biomaterials*, **33**, 3464 (2012).
29) S. M. Krug, et al.：*Biomaterials*, **34**, 275 (2013).
30) S. Masuda, et al.：*J. Cell Sci.*, **124**, 548 (2011).
31) T. Higashi, et al.：*J. Cell Sci.*, **126**, 966 (2013).
32) M. Furuse, et al.：*Ann. N. Y. Acad. Sci.*, **1257**, 54 (2012).
33) A. Tamura, et al.：*Gastroenterology*, **140**, 913 (2011).
34) D. W. Powell：*Am. J. Physiol.*, **241**, G275 (1981).

〈土山　遼／長瀬　翔太郎／
八木　清仁／近藤　昌夫〉

総説（Review Article）：膜（MEMBRANE），38（4），174-180（2013）

●特集　生体膜シンポジウム「生体防御の最前線：上皮バリアと輸送～基礎研究から創薬研究へ～」

Claudinを標的とした創薬研究の最前線

飯田愛未・八木清仁・近藤昌夫*

大阪大学　大学院薬学研究科
〒565-0871　大阪府吹田市山田丘1-6

The Cutting Edge of Claudin–targeted Drug Development

Manami Iida, Kiyohito Yagi, and Masuo Kondoh*

Graduate School of Pharmaceutical Sciences, Osaka University
1-6 Yamada-oka, Suita, Osaka 565-0871, Japan

Epithelial cells play pivotal roles in separating the body's internal environment from the outside environment. Ninety percent of malignant tumors are derived from epithelium, and most pathological microorganisms invade the body via the epithelial surface. Inflammatory conditions frequently disrupt the epithelial barrier. Epithelial cells are therefore potential targets for drug development. The first report of epithelial–cell–targeted drug development – namely, the use of EDTA to enhance the mucosal absorption of heparin – was published in *Nature* in 1961. However, the molecular basis of tight junctions, which are components of the epithelial barrier, has never been fully investigated, and this has led to a delay in epithelial–cell–targeted drug development. A series of studies by Dr. S. Tsukita has revealed that occludin and claudins are present in tight junctions. The claudins are a tetratransmembrane protein family with 27 members. The expression profiles of each member differ among tissues. Claudin–1, claudin–4, and claudin–5 are involved in the epidermal, mucosal, and blood-brain barriers, respectively. Claudin expression is deregulated in many malignant tumors. Claudin–1 is a co–receptor for hepatitis C virus. Claudin–4 is overexpressed in the epithelium covering mucosal immune tissues. Thus claudins are promising target molecules for drug development. In this review, we'd like to discuss the importance and future of claudin–targeted drug development.

Key words : claudin／tight junction／drug development

1. はじめに

約300年前，ドイツの観念哲学者ヘーゲルは，「事物のらせん的発展の法則」を提唱した．これは，事物の発展は直線的なものではなく，あたかもらせん階段を上るように発展していくという法則である．らせん階段を上る人を横から見ると上って行くように見えるが，上から眺めると元の位置に戻ってくる．即ち，事物の発展では，古く懐かしいものが新しい価値観を伴って再び現れてくると考えられている．

さて，周知のように薬物治療では上皮細胞における薬物透過が不可避であり，既に1950年代には粘膜上皮細胞を介した薬物吸収促進研究が開始されている．1960年代に入り隣接する上皮細胞間にタイトジャンクション（TJ）が存在，TJによって細胞間隙がシールされていることが示され，TJシール制御による薬物吸収促進法が開発され始めた．これが，TJを標的とした創薬研究の始まりである．

拙稿では，1960年代に生まれたTJを標的とした創

* Corresponding Author
Tel: +81-6-6879-8196
Fax: +81-6-6879-8199
E-mail: masuo@phs.osaka-u.ac.jp

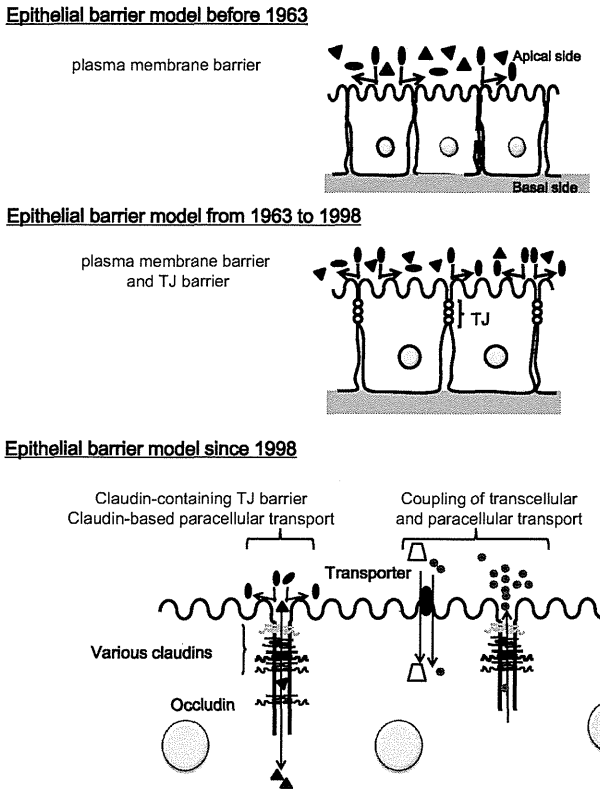

Fig. 1 Progression in paracellular transport research through understanding of the biology of the epithelial barrier.
The plasma membrane was originally considered to be the primary barrier in epithelial cell sheets. TJ strands were subsequently identified as the intercellular sealing components [33, 34]. Claudins were later found to be key structural and functional components of TJ seals. They function as intercellular seals and are also involved in the intercellular transport of ions. Claudins are coupled to both transcellular and paracellular transport. Claudin-based paracellular transport can be charge and size selective [12].

薬の萌芽が上皮細胞生物学の進展に伴い辿ってきたらせん的発展について，概説したい（Fig. 1）．

2. TJを標的とした創薬研究のはじまり

進化の過程において多細胞生物は，生体内外・組織内外を隔てる生体バリアとして上皮細胞を発達させてきた．薬物吸収ではこの障壁が透過・吸収障壁として機能することから，半世紀以上前から上皮細胞における薬物透過促進法の開発が進められ，1961年，Nature誌にEDTAが粘膜吸収促進作用を有しているという報告がなされている[1]．振り返るとこの論文がTJを標的とした創薬の端緒となっていたものの，当時はTJの存在が知られておらず，その作用機構は不明なままであった．1963年にTJが同定，1967年にTJシール制御による薬物吸収促進のproof of concept（POC）が確立され，粘膜上皮における透過促進活性を指標にした吸収促進剤の開発が進展していった[2,3]．

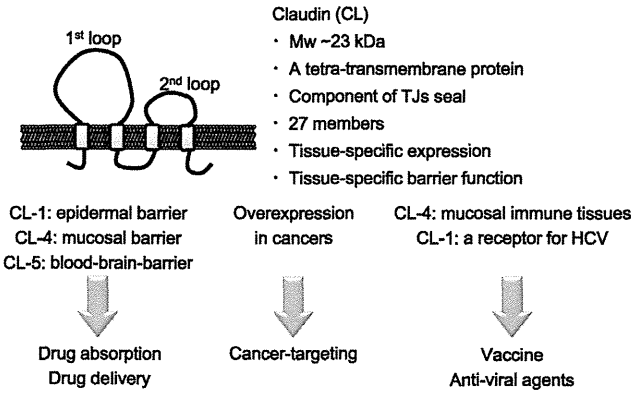

Fig. 2 Claudins as targets for drug development.

TJシール制御による薬物吸収のPOCが確立され，中鎖脂肪酸，ポリカチオンなどが吸収促進剤として研究開発されたものの，粘膜障害性を伴うこと，TJシール開口に伴う非特異的な物質流入が不可避であることから，臨床応用されているのはカプリン酸ナトリウム（C10）などに限られている．TJシールの分子基盤解析遅延に伴い，1990年代以降，安全性・特異性を兼ね備えた経細胞内経路（トランスポーターなどの利用）が上皮細胞の薬物透過研究のメインストリームとなった．

3. TJの分子基盤を標的とした創薬研究

上皮は生体内外を隔てるバリアとして機能しているのみならず，悪性腫瘍の90%は上皮由来であり，多くの病原性微生物は上皮を介して生体内に侵入する．さらに，炎症性腸疾患では上皮バリアは破綻しており，上皮は薬物吸収，薬物送達，癌，感染症，炎症性疾患に対する創薬ターゲットとして高い可能性を有している．しかしながら，ターゲット分子の解析遅延から，上皮を標的とした創薬研究の進展は立ち遅れていた．

Claudinの発見に端を発した上皮細胞生物学の進展に伴い，ヒトでは膵臓癌や膀胱癌をはじめとした12種類余りの癌でclaudinの高発現が認められること，粘膜免疫組織を覆う上皮細胞層にclaudin-4が高発現していること，claudin-1がC型肝炎ウイルス（HCV）の感染受容体の一つになっていること，炎症性腸疾

Table 1　Progressive elucidation of TJ biology

Year	Event
1963	Identification of TJ
1973	Identification of TJ strands
1982	*Membrane lipid hypothesis*
1986	Identification of ZO-1
1993	Identification of occludin
1998	Identification of claudin
1999 onward	Clarification of TJ barrier function of claudins
	Identification of paracellular ion transport via claudins
2011	Identification of transcellular transport coupled to claudin-based TJ strands

TJ: tight junction

患患者においてclaudinの発現異常が観察されることなどが報告され，TJの分子基盤claudinを標的とした創薬領域が拓きつつある（Fig. 2）[4〜7]．

3.1　吸収促進

TJの分子基盤については，1982年Nature誌に脂質ミセル説が提唱されたものの，10年余りにわたり構成成分すら未解明なままであった（Table 1）[8]．1993年に京都大学月田グループにより，TJ構成タンパク質として4回膜貫通タンパク質occludinが同定され，TJシールがタンパク質によって形成されていることが初めて実証された[9]．その後，occludinの細胞外領域ペプチドがTJのバリア機能を低下させること，マンニトールなどの透過性を亢進できることなどが見出され，TJシールの分子基盤を標的とした吸収促進法が提唱された[10]．しかしながら，occludinを欠損させてもTJシールに異常が観察されなかったことから，“真のTJシール分子基盤”の解析が進められ，1998年，TJを標的とした創薬研究のらせん的発展の起爆剤となるclaudinが，月田グループの古瀬らによって報告された[11]．Claudinは分子量約23 kDaの4回膜貫通タンパク質であり，現在までに27種類の分子が見出されており，claudin-1は皮膚バリア，claudin-5は血液脳関門，claudin-11は血液精巣関門を担っていることが明らかにされている[12,13]．

1999年にウエルシュ菌下痢毒素（CPE）の受容体がclaudin-3，-4と同一分子であること，CPEのC末側の受容体結合ドメイン（C-CPE）を上皮細胞に作用させると細胞障害性を伴うことなくTJバリア機能が減弱することから，claudin binderを利用した粘膜吸収の可能性が示唆された[14,15]．2005年には，C-CPEがカプリン酸ナトリウム（C10）の400倍余り

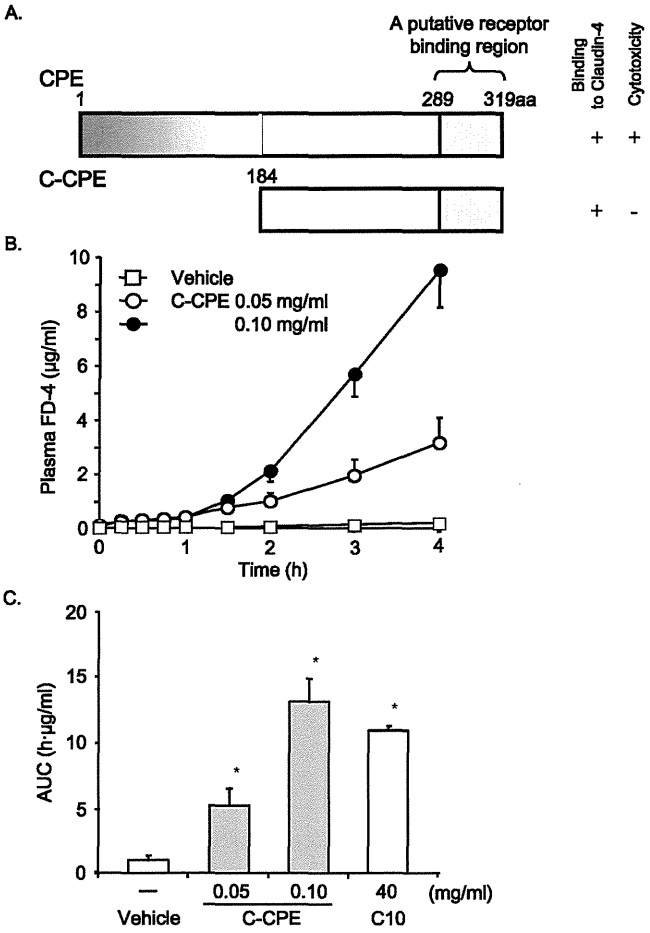

Fig. 3　Effect of C-CPE on jejunal absorption[16].
A) Diagram of CPE and C-CPE structures. C-CPE is the C-terminal fragment of CPE[35]. C-CPE binds to claudin-3/-4 and decreases TJ barrier function as indicated by a decrease in TER[15,36]. B, C) Effect of C-CPE on jejunal absorption in rats. Rat jejunum was treated with FD-4 (10 mg/ml) in the presence of vehicle, C-CPE or C10. The FD-4 levels in plasma were determined (B), and the area under the concentration curve between 0 and 4 h (AUC) was calculated (C). Data are means ± SE (n = 4). *Significant difference from the vehicle-treated group ($p < 0.05$).

の粘膜吸収促進活性を有すること，本吸収促進活性にはclaudin-4との相互作用が関与していることが示され，claudin binderを利用した粘膜吸収促進のPOCが確立された（Fig. 3）[16]．さらに，claudin binderは副甲状腺ホルモン（現在注射剤として使用）の経肺・経鼻吸収促進活性も有しており，claudinを標的としたバイオ医薬の非侵襲性投与法も提唱されている[17]．

TJシール開口作用を介して薬物吸収を促進する場合，薬物以外の物質の非特異的な流入が副作用発現

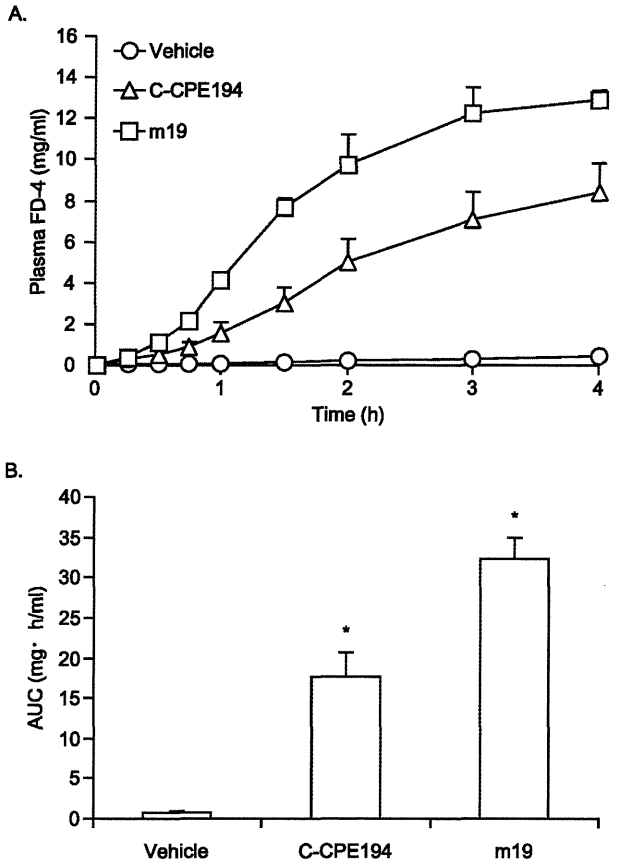

Fig. 4 Jejunal absorption–enhancing effect of C–CPE and m19[18]
Rat jejunum was treated with a mixture of 2 mg of FD–4 and 0.2 mg of C–CPE or m19. Time–course changes of plasma FD–4 level were monitored (A), and the area under the concentration curve between 0 and 4 h (AUC) was calculated (B). Data are means ± SE (n = 4). *Significantly different from the vehicle-treated group ($p < 0.05$).

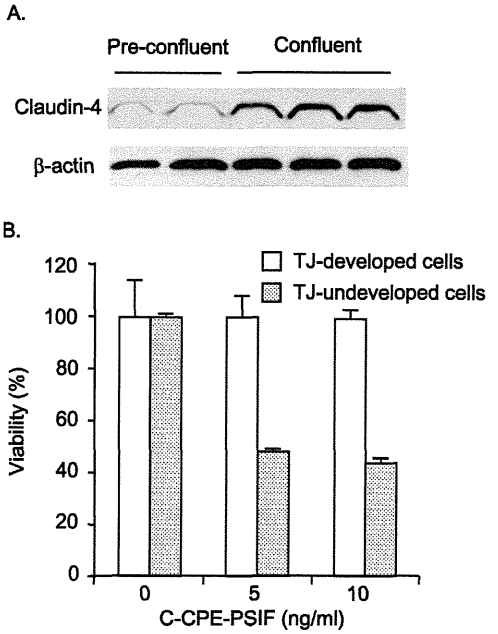

Fig. 5 Cytotoxic specificity of C–CPE–PSIF[23].
To develop tight TJs, Caco–2 monolayer cells were grown at confluency for 3 days. To maintain loose TJs, Caco–2 cells were seeded at sub–confluency. The cell lysates were subjected to SDS–PAGE followed by western blotting with anti–claudin–4 antibody (A). The cells were treated with the indicated concentrations of C–CPE–PSIF for 48 h, and then cell viability was measured by WST–8 assay (B). Data are means ± SD (n = 4).

に繋がる可能性が指摘されており，このことが細胞間隙経路を介した薬物吸収促進の実用化に立ちはだかる大きな壁となっている．TJには複数のclaudinが含まれていること，構成するclaudinの組合せによってTJシールとしての機能が異なること，claudinが細胞間隙経路を介したイオン透過に関与していること，claudin制御による物質透過に分子量依存性が観察されることから，claudinバリアを自由自在に制御することができれば，組織特異性および透過物質特異性を兼ね備えた新たな概念の吸収促進剤の開発が可能になると期待されている[12]．

実際，claudin–3, claudin–4は腸管に広く発現しているものの，C–CPEは空腸では粘膜吸収促進作用を示すが結腸では吸収促進活性を有していない[16]．さらに，C–CPEをprototypeとして作製された広域claudin binder（m19）は，C–CPEに比して優れた粘膜吸収促進活性を有しており，claudin阻害域を改変することで吸収促進特性を改変できる可能性がある（Fig. 4）[18,19]．

3.2 癌ターゲティング

2000年以降，悪性腫瘍（年間死者数700万人）の90%を占める上皮由来の癌とclaudinとの関連性についても多方面から研究が進み，卵巣癌，膵臓癌，膀胱癌等10種類以上の癌でclaudinの高発現が見出され，claudinが癌ターゲッティングの標的分子としても注目されている[5,20,21]．実際，claudin指向性毒素であるCPEは膵臓癌モデルに対して抗腫瘍活性を有しており，claudinを標的とした癌治療のPOCが確立された[22]．さらに，マウス乳癌細胞株4T1細胞を用いた担癌マウスモデルにC–CPEと緑膿菌由来のタンパク質合成阻害因子（PSIF）との融合タンパク質を投与したところ，体重減少を伴うことなく腫瘍増殖抑制効果が観察されていた．ヒト結腸癌細胞株であるCaco–2細胞はconfluent状態で培養すると正常上皮様の形態をとることが知られている．Sub–confluent状態の細胞を癌細胞，confluent状態の細胞を正常上

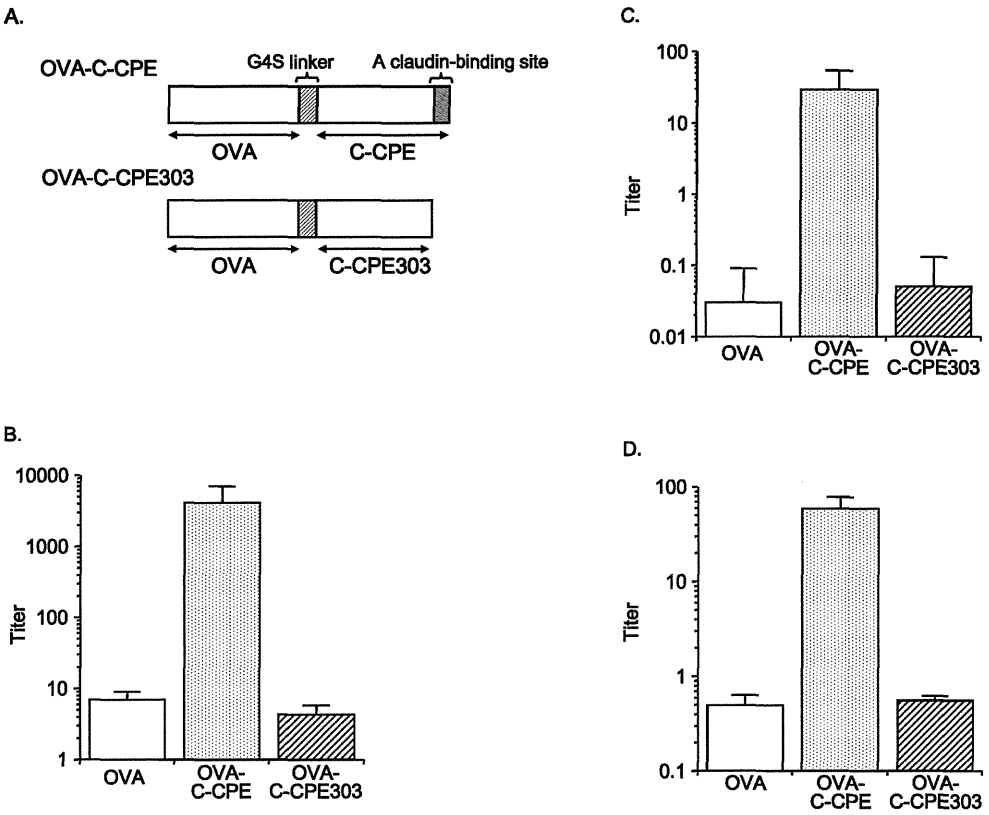

Fig. 6　Involvement of claudin–4 in immune responses to OVA–C–CPE[27].
A) Schematic illustration of OVA–C–CPE and its mutant. The C–terminal 16 amino acid–deleted C–CPE mutant (C–CPE303) did not bind to claudin–4[36]. To clarify the involvement of claudin–4 in the immune response initiated by OVA–C–CPE, OVA was fused with C–CPE303, resulting in OVA–C–CPE303. B–D) Immune responses by OVA–C–CPE or OVA–C–CPE303. Mice were nasally immunized with OVA, OVA–C-CPE, or OVA–C– CPE303 (5 μg OVA) once a week for 3 weeks. Seven days after the last immunization, the levels of OVA–specific serum IgG (B), nasal IgA (C), and vaginal IgA (D) were measured by ELISA. Data are means ± SD (n = 4).

皮細胞として用いた解析が行われ，confluent状態の細胞ではsub–confluent状態の細胞に比してclaudin–4発現レベルが高かったものの，C–CPE–PSIFに対する感受性が低下していたことから，claudin指向性分子は癌細胞特異的に作用するものと推察される(Fig. 5A and 5B)[23,24]．

正常な上皮細胞層では水平方向に細胞は分裂しコンタクトインヒビッションにより細胞増殖は制御されている．一方，上皮細胞が癌化すると，細胞の分裂軸が回転し垂直方向への分裂が始まり，コンタクトインヒビッションがかからず腫瘍組織を形成していくことから，この癌化早期イベントである分裂軸の回転を利用した癌治療戦略を構築することができれば，癌の早期診断・早期治療法の開発に繋がると考えられている[25]．分裂軸の回転に伴い，TJ構成タンパク質が管腔側に露出することから，claudinを標的とした癌治療戦略は癌の早期診断・治療法としての展開が期待される[20]．さらに，claudin binderにより腫瘍組織内の細胞間接着を弱めることで低分子抗癌剤の腫瘍内浸透性を改善できる可能性も指摘されており，claudinは癌ターゲティング療法のみならず，癌化学療法においても注目されつつある[20,21,26]．

3.3　粘膜ワクチン

昨今の新型インフルエンザの世界的流行でも明らかなように，依然として感染症は人類に立ちはだかる大きな脅威であり，感染症によって毎年2000万人の命が失われている．患者の生活の質（QOL）・有効性・安全性を考慮すると，非侵襲性投与が可能であること，多くの感染性病原体の侵入門戸（粘膜面）における防御網を構築できること，生体内に侵入した病原体の排除活性をも有することから，経鼻・経口ワクチンが理想的な感染予防法であると言える．しかしながら，消化酵素などによる分解を回避しつつ粘膜免疫組織に抗原を効率良く送達しなければならず，ここに粘膜ワクチン開発の難しさがある．2003年に東大医科研の清野グループにより，粘膜免疫組織にclaudin–4が高発現していることが見出さ

れ，claudin–4を標的とした粘膜免疫組織への抗原デリバリーの可能性が示唆された[7]．C–CPEとモデル抗原（卵白アルブミン）との融合タンパク質を経鼻免疫することで鼻粘膜IgAのみならず血清中IgG，糞便中IgA，膣粘膜IgA産生が認められること，C–CPEのclaudin結合ドメイン欠損体では抗体価の上昇が消失していたことから，claudinを標的とした粘膜ワクチンのPOCが確立された（Fig. 6A–6D）[27]．C–CPEは消化酵素耐性であることから，経口ワクチンへの応用も期待されている．

4. おわりに

上述したように，上皮細胞生物学の進展により，TJを標的とした創薬研究は，薬物吸収促進において質的な発展を遂げ，癌や感染症などへの展開も拓けつつある．本稿の最後に，TJを標的とした創薬研究の課題や展望についてふれてみたい．

TJシール制御による薬物送達では，細胞間隙経路の開口に伴う非特異的な物質の流入が実用化に向けた課題となっている．Claudinは27種類存在するメンバーの多種多様な組み合わせにより生体内の多様な内部環境維持に関与していると考えられており，claudinバリアを自由自在に制御する技術を構築することで透過物質特異的な薬物送達法の開発が可能になると期待されている．しかしながら，未だ本POCは確立されておらず，claudinバリア制御の安全性評価が焦眉の急となっている．

また，claudinを標的とした癌・ワクチン・C型肝炎治療法の顕在化では，claudin binderの創製が成否を握っているものの，claudinは細胞外領域が小さいうえにタンパク質精製が困難であり（現在のところ，claudin–4しか精製系が確立されていない），抗体を含めてclaudin binderの創製は立ち遅れている．ようやく最近，国内外の複数のグループにおいて，claudin遺伝子やclaudin発現細胞を免疫することでclaudinの細胞外領域を認識するモノクローナル抗体が創出され始めており，claudin binder創製技術が確立されつつある[26,28]．さらに，東大先端研の浜窪隆雄博士が開発した発芽バキュロウイルス（BV）を利用した膜タンパク質発現系を用い，claudin提示BVがclaudin binderスクリーニング系として機能することも見出されており，抗体作製技術と融合することでdruggable claudin binderの開発が進展していくものと期待される[29]．

京大月田グループによるoccludinおよびclaudinの発見に端を発した上皮細胞生物学の土壌に育まれ，TJを標的とした創薬研究は「吸収促進剤」から「経粘膜・経皮投与，癌治療，粘膜ワクチン開発，C型肝炎治療，脳内薬物送達，炎症性疾患治療」へとらせん的発展を遂げつつある．さらに，claudinが物質輸送系において細胞内経路と細胞間隙経路のカップリングに関与していること，免疫細胞の成熟化にclaudinが関与していること，claudin–5を標的とした外傷性脳損傷治療のPOCなども報告されており，TJを標的とした創薬研究の発展はとどまる気配を見せていない[30～32]．今後10年間のらせん的発展の行方を見据え，上皮細胞生物学の土壌に育まれた本邦発の創薬に向けた準備をしておくことは重要かもしれない．

謝　辞

本総説を執筆する機会を与えて頂いた浅野真司先生をはじめとした関係者の皆様方に衷心よりお礼申し上げます．

本稿で紹介させて頂いたデータの一部は，文部科学省科学研究費補助金（21689006; 24390042），厚生労働省科学研究費補助金，公益財団法人武田科学振興財団，公益財団法人中冨健康科学振興財団のサポートにより実施されたものであり，各助成機関に衷心よりお礼申し上げます．

文　献

1) Windsor E, Cronheim GE : *Nature*, **190**, 263-264 (1961)
2) Aungst BJ : *J. Pharm. Sci.*, **89**, 429-442 (2000)
3) Cassidy MM, Tidball CS : *J. Cell Biol.*, **32**, 685-698 (1967)
4) Evans MJ, von Hahn T, Tscherne DM, Syder AJ, Panis M, Wolk B, Hatziioannou T, McKeating JA, Bieniasz PD, Rice CM : *Nature*, **446**, 801-805 (2007)
5) Morin PJ : *Cancer Res.*, **65**, 9603-9606 (2005)
6) Schulzke JD, Ploeger S, Amasheh M, Fromm A, Zeissig S, Troeger H, Richter J, Bojarski C, Schumann M, Fromm M : *Ann. N. Y. Acad. Sci.*, **1165**, 294-300 (2009)
7) Tamagawa H, Takahashi I, Furuse M, Yoshitake-Kitano Y, Tsukita S, Ito T, Matsuda H, Kiyono H : *Lab. Invest.*, **83**, 1045-1053 (2003)
8) Kachar B, Reese TS : *Nature*, **296**, 464-466 (1982)
9) Furuse M, Hirase T, Itoh M, Nagafuchi A, Yonemura S, Tsukita S, Tsukita S : *J. Cell Biol.*, **123**, 1777-1788 (1993)
10) Wong V, Gumbiner B : *J. Cell Biol.*, **136**, 399-409 (1997)
11) Furuse M, Fujita K, Hiragi T, Fujimoto K, Tsukita S : *J. Cell Biol.*, **141**, 1539-1550 (1998)
12) Furuse M, Tsukita S : *Trends Cell Biol.*, **16**, 181-188 (2006)
13) Mineta K, Yamamoto Y, Yamazaki Y, Tanaka H, Tada Y, Saito K, Tamura A, Igarashi M, Endo T, Takeuchi K, Tsukita S : *FEBS Lett.*, **585**, 606-612 (2011)
14) Morita K, Furuse M, Fujimoto K, Tsukita S : *Proc. Natl.*

Acad. Sci. USA, **96**, 511-516 (1999)
15) Sonoda N, Furuse M, Sasaki H, Yonemura S, Katahira J, Horiguchi Y, Tsukita S : *J. Cell Biol.*, **147**, 195-204 (1999)
16) Kondoh M, Masuyama A, Takahashi A, Asano N, Mizuguchi H, Koizumi N, Fujii M, Hayakawa T, Horiguchi Y, Watanbe Y : *Mol. Pharmacol.*, **67**, 749-756 (2005)
17) Uchida H, Kondoh M, Hanada T, Takahashi A, Hamakubo T, Yagi K : *Biochem. Pharmacol.*, **79**, 1437-1444 (2010)
18) Matsuhisa K, Kondoh M, Suzuki H, Yagi K : *Biochem. Biophys. Res. Commun.*, **423**, 229-233 (2012)
19) Takahashi A, Saito Y, Kondoh M, Matsushita K, Krug SM, Suzuki H, Tsujino H, Li X, Aoyama H, Matsuhisa K, Uno T, Fromm M, Hamakubo T, Yagi K : *Biomaterials*, **33**, 3464-3474 (2012)
20) Kominsky SL : *Expert Rev. Mol. Med.*, **8**, 1-11 (2006)
21) Turksen K, Troy TC : *Biochim. Biophys. Acta.*, **1816**, 73-79 (2011)
22) Michl P, Buchholz M, Rolke M, Kunsch S, Lohr M, McClane B, Tsukita S, Leder G, Adler G, Gress TM : *Gastroenterology*, **121**, 678-684 (2001)
23) Saeki R, Kondoh M, Kakutani H, Tsunoda S, Mochizuki Y, Hamakubo T, Tsutsumi Y, Horiguchi Y, Yagi K : *Mol. Pharmacol.*, **76**, 918-926 (2009)
24) Saeki R, Kondoh M, Kakutani H, Matsuhisa K, Takahashi A, Suzuki H, Kakamu Y, Watari A, Yagi K : *J. Pharmacol. Exp. Ther.*, **334**, 576-582 (2010)
25) Wodarz A, Nathke I : *Nat. Cell Biol.*, **9**, 1016-1024 (2007)
26) Suzuki M, Kato–Nakano M, Kawamoto S, Furuya A, Abe Y, Misaka H, Kimoto N, Nakamura K, Ohta S, Ando H : *Cancer Sci.*, **100**, 1623-1630 (2009).
27) Kakutani H, Kondoh M, Fukasaka M, Suzuki H, Hamakubo T, Yagi K : *Biomaterials*, **31**, 5463-5471 (2010)
28) Fofana I, Krieger SE, Grunert F, Glauben S, Xiao F, Fafi-Kremer S, Soulier E, Royer C, Thumann C, Mee CJ, McKeating JA, Dragic T, Pessaux P, Stoll–Keller F, Schuster C, Thompson J, Baumert TF : *Gastroenterology*, **139**, 953-964 (2010)
29) Kakutani H, Takahashi A, Kondoh M, Saito Y, Yamaura T, Sakihama T, Hamakubo T, Yagi K : *PLoS One*, **6**, e16611 (2011)
30) Tamura A, Hayashi H, Imasato M, Yamazaki Y, Hagiwara A, Wada M, Noda T, Watanabe M, Suzuki Y, Tsukita S : *Gastroenterology*, **140**, 913-923 (2011)
31) Kawai Y, Hamazaki Y, Fujita H, Fujita A, Sato T, Furuse M, Fujimoto T, Jetten AM, Agata Y, Minato N : *Proc. Natl. Acad. Sci. U S A*, **108**, 4075-4080 (2011)
32) Campbell M, Hanrahan F, Gobbo OL, Kelly ME, Kiang AS, Humphries MM, Nguyen AT, Ozaki E, Keaney J, Blau CW, Kerskens CM, Cahalan SD, Callanan JJ, Wallace E, Grant GA, Doherty CP, Humphries P : *Nat. Commun.*, **3**, 849 (2012)
33) Staehelin LA : *J. Cell Sci.*, **13**, 763-786 (1973)
34) Farquhar MG, Palade GE : *J. Cell Biol.*, **17**, 375-412 (1963)
35) Katahira J, Inoue N, Horiguchi Y, Matsuda M, Sugimoto N : *J. Cell Biol.*, **136**, 1239-1247 (1997)
36) Takahashi A, Kondoh M, Masuyama A, Fujii M, Mizuguchi H, Horiguchi Y, Watanabe Y : *J. Control. Release.*, **108**, 56-62 (2005)

(Received 8 May 2013;
Accepted 23 May 2013)

著者略歴

飯田 愛未（いいだ まなみ）
2012年3月 大阪大学薬学部卒業
2012年4月 大阪大学大学院修士課程入学
現在に至る

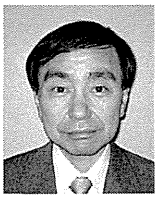

八木 清仁（やぎ きよひと）
1976年3月 大阪大学薬学部卒業
1980年9月 大阪大学大学院博士課程修了
1982年8月 米国メリーランド大学薬学部 研究助手
1984年2月～1985年3月 米国国立衛生研究所 客員研究員
1984年4月 大阪大学薬学部 助手
1992年4月 大阪大学薬学部 助教授
2000年3月 大阪大学大学院薬学研究科 教授
現在に至る

近藤 昌夫（こんどう ますお）
1994年3月 大阪大学薬学部卒業
1996年3月 大阪大学大学院修士課程修了
1998年3月 大阪大学大学院博士課程中退
1998年4月 徳島文理大学薬学部助手
2002年4月 昭和薬科大学 講師
2006年4月 大阪大学大学院薬学研究科 助教授
2007年4月 大阪大学大学院薬学研究科 准教授
現在に至る

Chihara et al. BMC Cancer 2013, 13:275
http://www.biomedcentral.com/1471-2407/13/275

BMC Cancer

TECHNICAL ADVANCE Open Access

Diagnostic markers of urothelial cancer based on DNA methylation analysis

Yoshitomo Chihara[1,2*], Yae Kanai[3], Hiroyuki Fujimoto[4], Kokichi Sugano[5], Kiyotaka Kawashima[6], Gangning Liang[7], Peter A Jones[7], Kiyohide Fujimoto[1], Hiroki Kuniyasu[2] and Yoshihiko Hirao[1]

Abstract

Background: Early detection and risk assessment are crucial for treating urothelial cancer (UC), which is characterized by a high recurrence rate, and necessitates frequent and invasive monitoring. We aimed to establish diagnostic markers for UC based on DNA methylation.

Methods: In this multi-center study, three independent sample sets were prepared. First, DNA methylation levels at CpG loci were measured in the training sets (tumor samples from 91 UC patients, corresponding normal-appearing tissue from these patients, and 12 normal tissues from age-matched bladder cancer-free patients) using the Illumina Golden Gate methylation assay to identify differentially methylated loci. Next, these methylated loci were validated by quantitative DNA methylation by pyrosequencing, using another cohort of tissue samples (Tissue validation set). Lastly, methylation of these markers was analyzed in the independent urine samples (Urine validation set). ROC analysis was performed to evaluate the diagnostic accuracy of these 12 selected markers.

Results: Of the 1303 CpG sites, 158 were hyper ethylated and 356 were hypo ethylated in tumor tissues compared to normal tissues. In the panel analysis, 12 loci showed remarkable alterations between tumor and normal samples, with 94.3% sensitivity and 97.8% specificity. Similarly, corresponding normal tissue could be distinguished from normal tissues with 76.0% sensitivity and 100% specificity. Furthermore, the diagnostic accuracy for UC of these markers determined in urine samples was high, with 100% sensitivity and 100% specificity.

Conclusion: Based on these preliminary findings, diagnostic markers based on differential DNA methylation at specific loci can be useful for non-invasive and reliable detection of UC and epigenetic field defect.

Keywords: Urothelial cancer, DNA methylation, Pyrosequencing, ROC, Piagnostic accuracy

Background

According to the American Cancer Society estimates for 2013, bladder cancer will account for 72,570 newly diagnosed cases and 15,210 deaths [1]. Bladder cancers can be classified into two groups based on histopathology and clinical behavior: non-muscle-invasive urothelial cancer (NMIUC: pTa-pT1) and muscle-invasive urothelial cancer (MIUC: pT2-pT4). NMIUCs represent approximately 80% of newly diagnosed bladder cancer cases and are treated by transurethral resection (TUR). However, 70% of the treated cases recur, and of these 15% progress to invasive cancers [2]. Consequently, the follow-up for NMIUC includes lifelong cystoscopy monitoring every few months. MIUC usually requires radical cystectomy and has a poor prognosis [3]. Although cystoscopy and cytology are the gold standard for diagnosing bladder cancer, cystoscopy is an invasive procedure and cytology has poor sensitivity for detecting low grade tumors [4]. It is therefore crucial to develop reliable and non-invasive early diagnostic markers to improve strategies for management of bladder cancer patients.

Genetic and epigenetic factors are known to contribute to the occurrence of bladder cancer [2]. Hence, several DNA-based urinary markers have been evaluated with the aim of reducing the need for cystoscopy and improving the accuracy of tumor detection. However, none have been proven to be sufficiently reliable in

* Correspondence: yychihara@gmail.com
[1]Department of Molecular Pathology, Nara Medical University, 840, Shijyo-cho, Kashihara, Japan
[2]Department of Urology, Nara Medical University, 840, Shijyo-cho, Kashihara, Japan
Full list of author information is available at the end of the article

detecting the entire spectrum of bladder cancers in the clinic [5].

Among the recently developed diagnostic markers for bladder cancers, those based on aberrant DNA methylation appear to be highly promising. Recent findings have indicated that epigenetic silencing associated with various cancers may involve DNA methylation extending over a large chromosomal region, often described as genome-overall hypomethylation or regional hypermethylation [6,7]. Diagnostic indicators based on DNA methylation have potential advantages over other genetic markers because DNA methylation occurs widely in cancer cells and consistently affects the same promoter regions. Therefore, a minimal analysis using a few loci is sufficient for diagnosis [8]. Furthermore, there is accumulating evidence that aberrant DNA methylation occurs frequently and early in human carcinogenesis [9,10]. Several studies on bladder cancer have indicated that tumor-specific DNA methylation markers have higher sensitivity and specificity than the parameters used in cytological urine analysis [11,12]. However, when used in highly sensitive, quantitative analytical techniques for measuring DNA methylation in urine samples, these markers tend to lose their both sensitivity and specificity for cancerous cells [13-15]. One of the reasons for this could be that aberrant DNA methylation occurs in non-cancerous tissue also due to aging, smoking and environmental factors [6]. Secondly, both cancer cells and normal transitional cells shed in the urine may have altered DNA methylation because of concomitant conditions, especially chronic inflammation and/or persistent infection [16], or the urine samples may be contaminated with other types of cells. Moreover, most studies analyzed a region within a CpG island (CGI) that may be altered in its methylation status, but may not affect gene expression in non-cancerous regions. Quantitative DNA methylation methods are advantageous as these can detect pre-malignant epigenetic field defects that cannot be revealed by histological examinations.

We previously reported aberrant DNA methylation occurring in urothelial cancer (UC) through a genome-wide approach [17]. The aim of the present study was to select and validate markers based on UC-specific regional aberrant DNA methylation. The association of UC with aberrant DNA methylation in selected loci was analyzed statistically by comparison of malignant and normal urothelial tissues. Lastly, we assessed the clinical relevance of the identified markers for detecting UC using urine samples.

Methods

Sample collection and preparation

Tissue samples were collected at 4 participating centers following protocols approved by an institutional review board: (1) University of Southern California, Norris Comprehensive Cancer Center, and 3 Japanese institutions, (2) Nara Medical University, Nara, (3) National Cancer Center Hospital, Tokyo, and (4) Tochigi Cancer Center Hospital, Tochigi. Informed consent was obtained from all participants at the respective institutions, and this study was approved by Nara Medical University Medical Ethics Committee as the project name "Epigenetic profiling and diagnostic markers of urogenital cancer based on DNA methylation analysis" from October 5, 2010.

Tissue samples of tumor and corresponding normal-appearing tissue adjacent to the tumor were obtained from UC patients during the surgical procedure (TUR or radical cystectomy). Corresponding normal-appearing tissue were judged macroscopically or endoscopically and dissected. A half of tissues were taken pathological examination, if the tissue included cancer, the section was excluded for the analyses. Control tissue samples of normal urothelia were obtained from patients without UC. Tumors were staged according to the UICC 1987 TNM Classification system [18]. All collected tissues were frozen and stored at −80°C until use for DNA extraction.

Urine samples were collected from UC patients before surgery and from healthy volunteers by spontaneous urination. Voided urine samples (50 mL) were centrifuged at 2000 × g for 10 min, and the pelleted urine sediment was rinsed twice with phosphate-buffered saline (PBS) and stored until use for DNA extraction.

DNA was extracted using conventional extraction methods [19]. DNA (2 μg) was treated with sodium bisulfite using Epitect Bisulfite Kit (Qiagen) according to the manufacturer's protocol and resuspended in 40 μL of distilled water for subsequent use.

Samples of urothelial tissue from UC patients (n = 144), adjacent normal appearing urothelia (n = 59) and patients without UC (n = 33) were divided into different experimental groups in order to generate sets for training and validation (Table 1). Samples of urine sediments from UC patients (n = 73) and healthy volunteers (n = 18) were analyzed as an independent validation sets. Samples collected from the 4 participating centers were distributed for identification of UC-specific DNA methylation and then for validation (Figure 1).

DNA methylation profiling using universal beads™ array

In our previous study, DNA methylation profiling was performed using the GoldenGate Methylation Cancer Panel I (Illumina Inc., La Jolla, CA) at the USC Epigenome Center [17]. In this study, the data were reanalyzed with the same platform for selected CpG sites from regions of aberrant DNA methylation specifically associated with tumors. The array interrogated 1,505 CpG sites selected from 807 cancer-related genes. The data were first

Table 1 Clinical characteristics of UC and control patients

	Training set	Tissue validation set	Urine validation set
Control patients (n = 51)	**12 (N)**	**21 (N)**	**18 (NU)**
Age, median (range) (years)	63 (50–80)	62 (27–82)	54 (16–77)
Male/female	12/0	13/8	6/12
UC patients (n = 217)	**91 (T)**	**53 (T)**	**73 (TU)**
Age, median (range) (years)	66 (40–91)	69 (49–85)	69 (36–88)
Male/female	80/11	42/11	59/14
Tumor-adjacent normal tissue*	**34 (CN)**	**25 (CN)**	-
Tumor Stage in UC patients			
Ta	20	2	7
T1	32	16	30
T2	13	9	24
T3	20	21	10
T4	6	5	2
Tumor Grade in UC patients			
G1	5	0	5
G2	38	25	32
G3	48	28	36

*Samples of normal-appearing tissue adjacent to the tumor were collected from UC patients for each set. Abbreviations: *N* normal urothelial tissue, *CN* corresponding normal-appearing tissue adjacent to the tumor in UC patients, *T* tumor tissue, *NU* urine sediments from healthy volunteers, *TU* urine sediments from UC patients.
Urothelial tissue samples were collected during surgical procedures from UC and control patients. Urine samples were collected from UC patients and healthy volunteers. Samples were divided into experimental groups as given.

analyzed using the BeadStudio Methylation software (Illumina Inc., La Jolla, CA), and then a supervised cluster analysis with correlation metrics and average linkage was carried out using the open-source program Cluster 3.0. A β value of 0 to 1.0 was reported for each CpG site signifying percent methylation from 0-100%, respectively. The β values were calculated by subtracking background using negative control on the array and calculating the ratio of the methylated signal intensity to the sum of both methylated and unmethylated signals plus a constant of 100. Measurements with detection $p > 0.05$ were marked missing.

Bisulfite pyrosequencing

DNA methylation status of candidate tumor-specific hyper- or hypo-methylated CpG sites was assessed by pyrosequencing (PSQ) using Pyrosequencing 96HS (Biotage, Uppsala, Sweden) and PyroMark Q24 (Qiagen) according to the manufacturer's protocol. To enable single-strand preparation, the reverse primer was 5′-biotinylated. Reaction volumes of 30 μl contained 5× GoTaq buffer, 1.5 units GoTaq Hot Start Polymerase (Promega), 1 μM of primers, and 500 nM of dNTPs. PCR conditions were as follows: 95°C for 3 min; 45 cycles of 95°C for 30 s, the respective annealing temperature for 30 s, and 72°C for 30 s; and a final extension step at 72°C for 4 min. PCR primer sequences are given in Table 2. PSQ primers were designed to include CpG or near-CpG regions within 300 bps that were assayed on the Illumina GoldenGate Panel.

Immunohistochemistry

The immunohistological studies of *SOX1*, *TJP2*, *VAMP8* and *SPP1* were carried out on formalin fixed, paraffin embedded tissue samples, of which 5 normal tissues and 53 tumor tissues in the training set as described previously [19]. The primary antibodies were polyclonal rabbit anti-SOX1 (Abcam Inc., diluted at 1:500), polyclonal rabbit anti-TJP2 (kindly provided by Dr. Masuo Kondo, Graduate School of Pharmaceutical Sciences, Osaka University, Japan), monoclonal rabbit anti-VAMP8 (Abcam Inc., diluted at 1:100) and monoclonal rabbit anti-SPP1 (Abcam Inc., diluted at 1:100). Immunoreactivity was evaluated according to modified Allered's score system [20]. Briefly, the score represented the estimated proportion of positively stained cells (0 = none, 1 = less than 1/100, 2 = 1/100 to less than 1/10, 3 = 1/10 to less than 1/3, 4 = 1/3 to less than 2/3, and 5 = 2/3 or above). The staining intensities were averaged from the positive cells (0 = none, 1 = weak, 2 = intermediate, and 3 = strong). The product of these scores served as the total score. All results were scored by one of the authors (H. K.) without prior knowledge of the DNA methylation status.

Statistical analysis

Graphpad Prism version 4.02 was used for performing the Mann–Whitney *U* test, calculating receiver operating characteristics (ROC) for sensitivity and specificity of the candidate loci and Pearson's correlation coefficient.

Results

Identification of candidate UC-specific aberrant DNA-methylated CpG Sites

In our previous study, differentially methylated regions had been identified in DNA samples from normal and UC urothelial tissues [17]. In the present study, as a first step, tumor-specific, aberrant DNA methylation sites were identified within CpG loci. DNA methylation profiling was compared between 3 groups of tissue samples (Figure 2): normal urothelial tissue (N, n = 12), corresponding normal-appearing tissue adjacent to the tumor in UC patients (CN, n = 34), and tumor samples saved

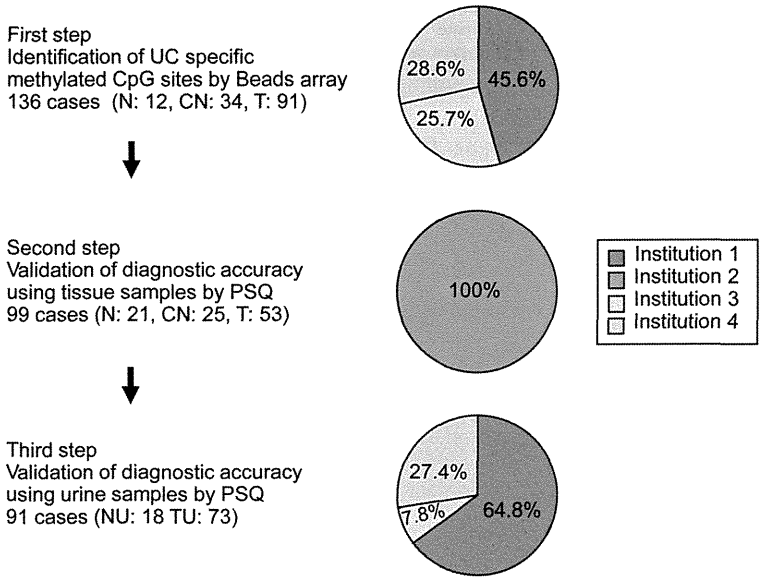

Figure 1 Study design. Samples of urothelial tissues and urine collected at the indicated participating centers and distributed for identification of UC-specific DNA-methylation sites (**First step**) and validation of diagnostic accuracy (**Second and Third steps**) as indicated. N: normal urothelia, CN: corresponding normal-appearing tissue adjacent to tumor from UC patient, T: tumor samples from UC patients; NU: urine from normal participants, TU: urine from UC patients treated by transuretheral resection; PSQ: pyrosequencing. Institution 1: Department of Urology, Norris Comprehensive Cancer Center, University of Southern California. Institution 2: Urology Division, National Cancer Center Hospital, Tokyo. Institution 3: Department of Urology, Nara Medical University. Institution 4: Department of Urology, Tochigi Cancer Center Hospital.

during TUR procedure on UC patients (T, n = 91). The tumor samples were further stratified based on tumor staging into NMIBC and MIBC (Figure 2). X-linked CpGs and those with a poor signal (defined by a detection p-value of >0.05) were eliminated, which left 1,303 sites for analysis (Additional file 1: Table S1). A supervised cluster analysis of N versus CN and T samples revealed UC-specific DNA methylation alterations, of which 158 were hypermethylated CpG sites and 356 were hypomethylated sites ($p < 0.001$) (Figure 2, Additional file 2: Table S2). In these loci, we selected top 30 CpG sites from the statistical results which showed lesser p-value both between N and CN, also CN and T. We verified DNA methylation status using the same training sets by PSQ and compared with GoldenGate data. Finally, we identified the 12 CpG sites (5 were hyper methylated and 7 were hypomethylated) from 11 genes, of which quantification of DNA methylation status were well accorded with GoldenGate data (Table 3). We also identified the top 13 CpG sites which distinguished N from CN. Then PSQ was performed on DNA samples allocated to the tissue validation set (Table 1: 21Ns, 25 CNs and 53 Ts) and urine validation sets (Table 1: 18 urine sediments from healthy volunteers (NUs) and 73 urine sediments from UC patients (TUs)).

Diagnostic accuracy of DNA methylation markers of UC

In the next step, the sequence-verified loci were tested for diagnostic accuracy by ROC analysis. To determine the diagnostic accuracy for UC tumors, T versus N/CN analysis was performed on 12 CpG loci from 11 genes, of which 5 loci were hypermethylated and 7 hypomethylated (Table 3). The cut-off values to discriminate T from N/CN using each marker were determined from the ROC curves as the maximum values of sensitivity and specificity, as follows: [sensitivity (%) + specificity (%) – 100]. For all 12 loci, there was a statistically significant and dramatic distinction in DNA methylation levels between N/CN and T. The ranges for area under the curve (AUC), sensitivity and specificity were 0.85–0.97, 75.0–94.34% and 84.44–100% respectively (Table 3). In particular, combination analysis of *SOX1* and *VAMP8* could distinguish T from N/CN with 100% sensitivity and specificity (data not shown). Interestingly, DNA methylation levels in CN samples were not correlated with their respective T samples, and DNA methylation levels in T samples did not correlate with age, gender and stage for all 12 markers.

To determine the diagnostic accuracy of epigenetic field defect, ROC analysis was performed for the tissue samples, N versus CN, using 13 markers from 13 genes, of which 10 were hypermethylated and 3 hypomethylated

Table 2 Primer sequences for PSQ

Gene	Annotation	Forward	Reverse	Sequencing	Sequence analyzed	Amplicon location relative to transcription start site
SOX1	Sex determining region Y box1	GGTATTTGGGATTAGTATATGTTTAG	CTATCTCCTTCCTCCTAC	TTAGTATATGTTTAG	CGTACGCGGCGCGTCG	-462~ -351
TJP2	Tight junction protein 2	GGTTTTTAGATAGGATTTAAAATTTTGAG	CAAAACCTCACACAAACAACTTC	AGGTTTTTTTAGTT	CGATTTTTCG	-492~ -409
MYOD1	Myogenic differentiation 1	GTGGGTATTTAGATTGTTAGTA	ACAATAACTCCATATCCTAAC	GAAGTTAGGAT	CGTGTCGCGTTATCG	+96~ +233
HOXA9_1	Homeo box A9	TTGTTTAATTTTATGTGAGGGGTTT	CAAATCTAACCTTATCTCTATACTCTCCC	TGATATAAAATAGTT	CGTTTAAG	-397~ -243
HOXA9_2	Homeo box A9	ATGAAATTTGTAGTTTTATAATTTT	ATTACCCAAAACCCCAATAATAAC	GTTTTATAATTTT	CGTGGGTCGGGTCGGGCGG	+10~ +100
GALR1	Galanin receptor 1	ATTAATGGA TGAGGAGGTT	ATACCAAAAA CTTCTCTACT AC	GTGATTTTTA AGGGG	CGCGGATTTT AGTCGAGTTG	-194~ +110
IPF1	Insulin promoter factor 1	GTAGTTTTAA GAGGAAGG	AAAAATTAAA ACCCATTTAA CCAA	GTAGTTTTAA GAGGAAGGT	CGCGTTTTTTTTTTCGTTG	-786~ -702
TAL1	T-cell acute lymphocytic leukemia 1	GTAAATAGAA GGAGGTTTT	ACACTACTTT CAAAAATATA AC	AGAA GGAGGTTTT	CGTAG TTAATTTAAG ATTTCG	-613~ -470
EYA4	Eyes absent homolog 4	GGATGTTTTGTTTTTATTAGAGGTATAG	AATTCTCTCAACTCAAACTCCC	GAAGGGGAAATTT	CGATATTGGAAGGAACG	+252~ +457
CDH13	Cadherin 13	AGTTTAAAGAAGTAAATGGGATGTTA	CTTCCCAAATAAATCAACAACAAC	ATTTGTTATGTAAAA	CGAGGGAGCGT	-175~ +6
CYP1B	Cytochrome P450 family 1	GTTTTGATTTTGGAGTGGGAGT	CTACCCTTAAAAACCTAACAAAATC	AGGGTATGGGAATTGA	CGTTATTTATCGA	+26~ +178
NPY	Neuropeptide Y	GGGTTGTTTT TATTTTTGGT AGGATTAGA	CACCAAAACC CAAATATCTA CCC	AGGAAAGTAGGGAT	CGGGT ATTGTTCGAG	-353~ -253
VAMP8	Vesicle-associated membrane protein 8	AAGTTTTTGT TTGGGAAGTT ATT	CATATCTCAA AACAACCCAA	GTTAGGTGTG GTTGGAG	CGATTCGAGATGCGAGGTGG	-157~ +56
CASP8	Caspase 8	GAAGTTTGATTTTGTTGGTTTAAAA	CAACCTCTCTAACTAAACCCTCCTT	TGTTTAGAGGTTG	CGGGTTGCGGGT	+431~ +533
SPP1	Secreted phosphoprotein 1	GGAATAAGGA TAGGTAGGT	CAAAATAACT ACTTAAAAAA ACTACTTCAA	GAATAAGGAT AGGTAGGTTG GG	CGATTTGTTTAAGGTTGTAT	+99~ +117
CAPG	Capping protein	GGGGTAGGTTGGAAGGAAGA	ACAACCACCCTACCACCTTCA	GTTGGAAGGAAGA	CGAATTTACGAAGT	+200~+294
RIPK3	Receptor-interacting serine-threonine kinase 3	GTTTTTGGAA GGTGAGGAT	AAAACTAATA CCTTTCTCCT TAACT	ATTTAATT TGGTTG	CGGT AGGTGTTTAG GAAACG	-137~ -27
IFNG	Interferon gamma receptor 1	AATAGTATTTGTTTGTGGTTGAA	TAACACCAAATCTCAAAATAACT	GAAAATGATTGAATAT	CGATTTG	+257~ +359
HLADPA1	Major histocompatibility complex, class II, DP alpha 1	AATTTTGAAAATGAATTGTGAATTG	CATTCTCTATTACTAAATAAAAAAAAC	GAGTTTTTTTGATTA	CGTTGGTA	-74~ +38

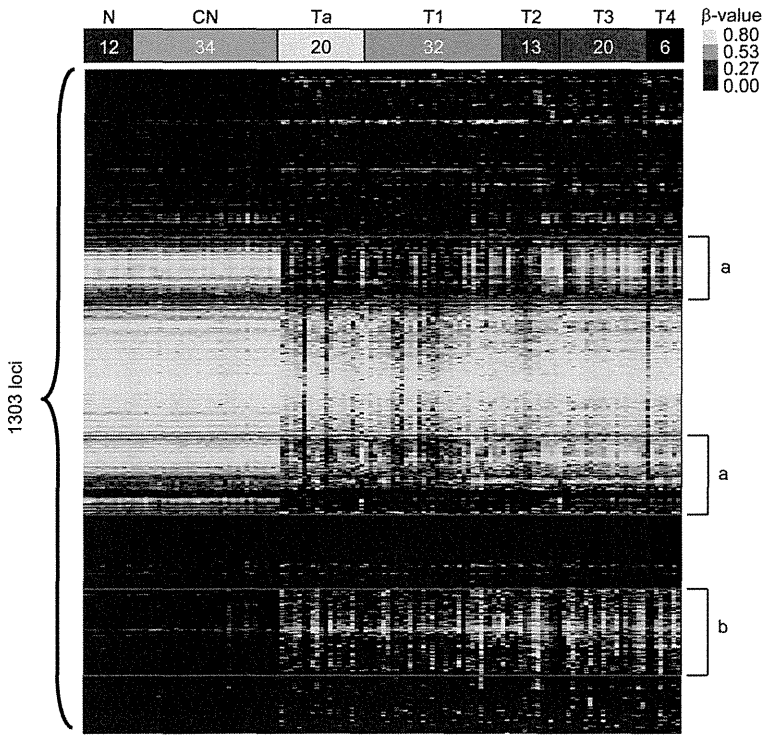

Figure 2 Global DNA methylation alterations in UC. Supervised cluster analysis of 1,303 loci (784 genes) from bladder samples, using the Illumina GoldenGate methylation assay. N (n = 12) represents normal tissue from patients without urothelial cancer (UC); CN (n = 34) represents corresponding normal-appearing tissue from UC patients; Ta-T1 (n = 49) represents non-muscle-invasive bladder cancer; and T2-T4 (n = 38) represents muscle-invasive bladder cancer. No methylation is shown in blue, and increasing DNA methylation is shown in yellow. (**a**) UC-specific hypomethylated CpG sites, and (**b**) UC-specific hypermethylated CpG sites.

(Table 3). The ranges for AUC, sensitivity and specificity were 0.73–0.93, 56.0–88.0%, and 71.43–100%, respectively (Table 3).

Diagnostic accuracy for UC as measured by DNA methylation in urine samples was evaluated based on the same 12 loci as for tissue samples, and determined by ROC analysis on NU versus TU urine samples. For all 12 markers, DNA methylation levels in TUs were statistically significantly distinct from those in CUs. The ranges of AUC, sensitivity and specificity were 0.67–0.93, 41.54–97.06%, and 40.0–100% respectively (Table 3). Among the loci examined here, values for AUC corresponding to urine samples were lower than those corresponding to urothelial tissues, except for the loci *MYOD* and *HOXA9_1*. Also the cut-off value which distinguishes TU from NU in both hyper- and hypo- methylated markers were lower in urine than in the tissue for all cancer types, except in *IFNG*. These results suggested that either the copy number of methylated CpG loci in urine sediments was difficult to be detected because of low DNA quality, or the concentration of cancer cells were diluted by the presence of other unrelated cells in the urine.

Representative scatter plots for 2 hypermethylated loci (*SOX1* and *HOXA9_2*) and 2 hypomethlated loci (*IFNG* and *SPP1*) examined in the various tissue and urine samples are shown (Figure 3).

The DNA methylation data were analyzed for each tissue/urine sample to determine the number of loci for which a given sample was considered a true positive based on the respective cut-off value (Table 4). Thus, out of the 53 T samples, 50 were positive for at least 6 and more loci. On the other hand, there were 3 T samples that were false negative for some loci and there was 1 N/CN sample that was false positive for some loci. Most tumor samples were positive for at least 6 markers. In other words, true-positive levels of DNA methylation for 6 or more markers allowed clear discrimination between T and N/CN samples with 94.3% sensitivity and 97.8% specificity (Table 4 top). For distinguishing between cancerous and non-cancerous tissue, the 13 loci selected for comparing N (n = 21) with CN samples (n = 25) were examined for each tissue sample. All the normal samples were positive for a maximum of 6 loci, while a majority of the CN samples were positive for at least 8 loci. Hence, for samples that showed altered DNA methylation for 7 or more markers, N could be discriminated from CN with 76.0% sensitivity and 100% specificity (Table 4 middle; false negative: 6/25; false positive: 0/21). In the case of

Table 3 ROC analysis of DNA methylation markers for UC

Gene	Cut-off value (%)	AUC	Sensitivity (%)	Specificity (%)	P value
Validation in tissue (N/CN vs. T)					
Hypermethylation					
SOX1	32.59	0.97	93.62	97.5	5.13E-14
TJP2	71.42	0.92	84.91	97.78	1.19E-12
MYOD	26.0	0.91	75.0	79.83	1.73E-12
HOXA9_1	55.59	0.86	76.6	97.83	9.00E-08
HOXA9_2	29.06	0.86	83.02	97.83	5.22E-10
Hypomethylation					
VAMP8	12.5	0.96	94.34	97.83	2.22E-15
CASP8	23.18	0.96	94.34	95.65	4.88E-15
SPP1	26.14	0.95	86.79	100	1.49E-14
IFNG	64.7	0.93	82.98	95.65	2.16E-12
CAPG	16.21	0.93	83.02	95.65	1.08E-12
HLADPA1	14.31	0.88	84.62	86.96	1.06E-09
RIPK3	22.97	0.85	81.63	84.44	9.54E-07
Validation in tissue (N vs. CN)					
Hypermethylation					
SOX1	16.51	0.86	68.18	100	9.04E-05
MYOD	12.71	0.85	76.0	85.71	5.19E-05
HOXA9_1	22.95	0.80	76.0	80.95	0.00043
GALR1	7.24	0.85	76.0	85.71	4.26E-05
IPF1	33.83	0.74	64.0	76.19	0.0089
TAL1	29.47	0.83	76.0	85.71	0.00011
EYA4	6.38	0.80	83.33	73.68	0.0078
CDH13	7.13	0.93	88.0	85.71	5.24E-07
CYP1B	13.61	0.75	60.0	80.95	0.0040
NPY	10.31	0.82	88.0	71.43	0.00018
Hypometylation					
CASP8	46.38	0.73	60.0	85.71	0.0084
IFNG	84.93	0.78	56.0	95.24	0.001
HLADPA1	24.27	0.83	72.0	85.71	0.00011
Validation in urine sediment (NU vs. TU)					
Hypermethylation					
SOX1	15.62	0.74	41.54	100	0.0041
TJP2	7.933	0.79	92.54	56.25	0.0003
MYOD	9.897	0.93	86.79	87.50	3.10E-05
HOXA9_1	7.038	0.92	86.23	88.89	4.25E-05
HOXA9_2	3.20	0.81	88.57	61.54	0.0004
Hypomethylation					10.78
VAMP8	10.78	0.72	97.06	40.0	0.023
CASP8	7.863	0.82	73.61	76.92	0.0005
SPP1	21.23	0.79	85.94	75.0	0.0015
IFNG	86.08	0.76	55.07	92.31	0.0037
CAPG	8.08	0.67	83.82	56.25	0.04
HLADPA1	6.46	0.82	77.19	90.0	0.0009
RIPK3	9.37	0.75	82.35	70.0	0.011

Selected loci that were identified as either hyper- or hypo-methylated were analyzed for their degree of DNA methylation and association with UC. The loci are named by the genes in which they occur; if there are 2 loci in the same gene, the suffixes 1 and 2 are added.

urine samples, the 12 loci with altered DNA methylation were examined for each sample of the NU (n = 18) and TU (n = 73) groups (Table 4 bottom). The distinction between the 2 groups was clear as there were no false positives or false negatives and all TU samples were positive for at least 6 loci. Thus, in the case of samples that showed true-positive levels of altered DNA methylation in 6 or more loci, discrimination between TU and NU samples was possible with 100% sensitivity and 100% specificity.

Correlation of the genetic expression with DNA methylation status

To evaluate epigenetic gene regulation of UC-specific aberrant DNA-methlated CpG sites, we made a comparison between DNA methylation levels and genetic expression on 2 hypermethlated and 2 hypomethylated markers. In hypermetylated genes, *SOX1* expression decreased in tumor tissues significantly (p = 0.0107). However DNA methylation levels did not correlate with gene expression (Additional file 3: Figure S1). On the other hand, gene expression of 2 hypomethlated genes significantly increased in tumor tissues. Furthermore DNA methylation levels of *SPP1* inversely correlated with gene expression significantly.

Discussion

Earlier studies have shown distinct DNA methylation patterns between UC and normal tissues, which could serve as useful indicators of early stages in the multistep process of carcinogenesis in UC [9,10]. Further, urothelial tissues affected by UC could be clearly distinguished from normal urothelia based on the presence of aberrant DNA methylation regions in cancer-associated genes such as *CDH1* [21], *RASSF1A* [11] and *RUNX3* [22] with sufficient sensitivity and specificity. However, to diagnose UC via analysis of a urine sample, a combination of several DNA methylation markers would be required to ensure high accuracy. Hence, the aberrant DNA methylation status of previously reported UC-associated genes alone would not provide sufficient accuracy with high sensitivity and specificity. On the other

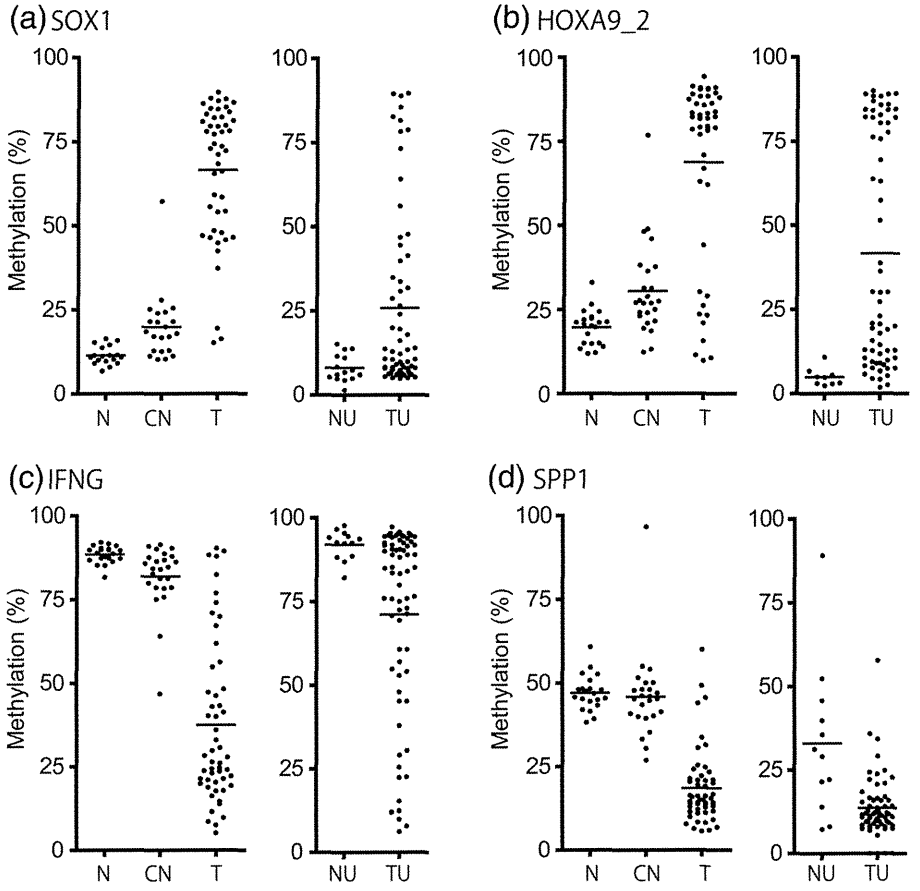

Figure 3 Differential DNA methylation at CpG sites. Scatter plots of quantitative DNA methylation analysis by PSQ in select loci that were hypermethylated: (**a**) *SOX1* (**b**) *HOXA9_x2*; or hypomethylated: (**c**) *IFNG* (**d**) *SPP1*. Mann–Whitney *U* test was used to compare quantitative methylation levels between the 2 groups. Short horizontal lines represent the median.

hand, increasing the number of markers increases the sensitivity, albeit at the cost of specificity.

In this study, we identified a panel of loci with UC-specific alterations in DNA methylation. The study design included 3 steps for identification and validation of these loci analyzed in urothelial tissue or urine samples (Figure 1). In the first step, high-throughput DNA methylation profiling revealed a total of 514 CpG sites that caused UC-specific aberrant methylation with statistical significance ($p < 0.001$). This corresponds to 39.4% of CpG sites assayed by the Bead™ array and suggested genome-wide UC-specific DNA methylation. Furthermore, normal tissue and normal-appearing tissue adjacent to UC patients were found to be significantly different with regard to 39 hypermethylated sites and 7 hypomethylated sites. These CpG sites could also be used to diagnose UC risk. (data not shown). These results indicated that aberrant DNA methylation in UC already occurred in non-cancerous epithelia in UC patients, supporting the notion that DNA methylation alterations occur gradually during the multistep process of carcinogenesis.

The DNA methylation status of the various CpG sites identified from Bead™ array data as UC-specific was sequence verified by PSQ. Next, we evaluated the diagnostic accuracy of 12 CpG sites. Interestingly, most of these loci were in genes that have not been reported for their aberrant DNA methylation in UC, except *CASP8* [23]. Since these CpG sites were identified from the clustering data in the comparison of normal and cancerous tissues, DNA methylation levels assayed by PSQ represented the fraction of methylated DNA clones in a sample, proportional to the number of malignant cells, if the tumor heterogeneities are ignored. In the tissue analysis, DNA methylation level between N/CN and T could be clearly discriminated for each marker, and the combination analysis of all 12 markers provided accuracy, 94.3% sensitivity, and 97.8% specificity (Table 4). Furthermore, CN could be discriminated from N with 76.0% sensitivity and 100% specificity. These results indicate that UC-specific aberrant DNA methylation also occurred in the adjacent normal epithelia, but at a lower level than in the tumor. In this way, the quantitative

Table 4 Diagnostic accuracy of the panel markers for UC

	Aberrant methylation		Sensitivity (%)	Specificity (%)
	Less than 5	6 and more		
N/CN	45	1	94.3	97.8
T	3	50		
	Aberrant methylation		Sensitivity (%)	Specificity (%)
	Less than 6	7 and more		
N	21	0	76	100
CN	6	19		
	Aberrant methylation		Sensitivity (%)	Specificity (%)
	Less than 5	6 and more		
NU	18	0	100	100
TU	0	73		

Abbreviations: *N* normal urothelial tissue, *CN* corresponding normal-appearing tissue adjacent to the tumor in UC patients, *T* tumor tissue, *NU* urine sediments from healthy volunteers. *TU* urine sediments from UC patients.

methylation analysis has an advantage in detecting field defect, which is a useful indicator for determining UC risk or predicting recurrence. Aberrant DNA methylation of *TJP2*, *SPP1*, and *IFNG* did not show a statistically significant difference between N and CN (data not shown), although these epigenetic alterations are thought to be cancer-specific and a part of the multistep carcinogenesis. Interestingly, *TJP2* (tight junction protein) is located on chromosome 9 (9q21.11), which shows allelic loss in UC most frequently. Allelic loss on chromosome 9 was thought to be the earliest genetic event arising in UC; however, we previously reported that allelic loss on 9q had not occurred in tissue showing dysplasia and adjacent normal urothelia of UC patients [19]. Taking into consideration these genetic and epigenetic alterations in adjacent normal urothelia, the alteration on 9q might be a truly tumor-specific event.

In the urine analysis, the combination of 12 markers provided sufficient accuracy to discriminate TU from NU, with 100% sensitivity and 100% specificity, and indicated a higher detection value for UC than so far reported for DNA methylation marker panels using quantitative analysis [13,14]. However, compared with the tissue analysis, the diagnostic power of each marker was not sufficient, and data from all 12 markers were required for a true diagnosis.

To determine whether the aberrantly methylated loci might play a functional role in tumorigenesis, we compared 4 genes expression to DNA methylation levels. In our results, a hypermethylated gene, *SOX1* expression reduced in tumor tissue, whereas *TJP2* expression did not reduce. In a recent study by Dudziec E. et al. [24], a large scale profiling among DNA methylation, histone modification and gene expression using UC cells revealed that 20-30% genes were silenced by epigenetic regulation. In this way, aberrant regional hypermethylation in cancer cells do not always regulate gene expression, and the hypermethylated loci that identified in this study might be a hallmark of cancer. In contrast to promoter hypermethylation, hypomethylation-dependent transcriptional activation in cancer is less frequent [25]. Currently, major contribution of global hypomethylation especially in retrotransposons and pericentromeric repeats are thought to be the enhancement of genomic instability [26]. Interestingly, hypomethylation of *VAMP8* and *SPP1* correlated with the gene expression significantly. Furthermore DNA methylation levels of *SPP1* inversely associated with expression levels. Several studies showed some transcription control regions, with the hypormethylated and activated in cancer [27,28] (Although we examined only 4 genes, our results might support these phenomena. Further studies needs to clarify the association aberrant DNA methylation with gene expression in cancer.

A limitation of this study is that candidate UC-specific DNA methylation loci were identified using tissue samples in the first step, and these markers showed a poorer diagnostic sensitivity in urine than in tissue samples. However, urine sediments from the healthy population sometimes show aberrant DNA methylation that is unrelated to cancer, and cluster analysis to identify DNA methylation loci by just urine samples may reflect the etiology of UCs. Another limitation is small numbers of each step. Also the consecutive concordant study that revealed DNA methylation status of T, CN and TU samples in one person including follow-up urines.

Conclusions

In conclusion, by a genome-wide analysis, markers based on DNA methylation were identified for high accuracy of diagnosis of UCs using urine samples in our preliminary study. These markers will need to be validated in a larger scale study. In the future, it may be possible to develop a panel of carefully selected DNA methylation markers for use on urine sediments to detect both primary UCs and recurrent UCs. In this way, DNA methylation profiling might be a useful tool to discriminate several clnicopathological factor of UCs and to clarify the multi-step carcinogenesis of UCs.

Additional files

Additional file 1: Table S1. All data of universal beads™ array.

Additional file 2: Table S2. Aberrant DNA methylated loci obtained from beads™ array.

Additional file 3: Figure S3. Correlation between gene expression and DNA methylation levels in normal and UC tissues.Five normal urothelial tissues (N) and 53 tumor tissues (T) (Stage, Ta: 13, T1: 21, T2: 7, T3: 10, T4: 2, Grade, G1: 2, G2: 25, G3: 26) were analyzed. Immunohistocheistry (IHC)

(left) represents corresponding median IHC score in each group. Original magnification, ×200. Expression of 4 genes in normal and tumor tissues were shown in Scatter plots (middle). Mann–Whitney *U* test was used to compare quantitative methylation levels between the 2 groups. Short horizontal lines represent the median. Pearson's correlation coefficient between IHC score and DNA methylation levels (right). Blue circles represent normal tissues.

Competing interests
The authors declare that they have no competing interests.

Authors' contributions
YC conceived of the study, participated in its design and coordination and drafted the manuscript. YK and HF collected UC samples and gain ethics committee approval to enroll this study at National Cancer Center Hospital Tokyo Japan. YK also helped to performed PSQ experiments. KS and KK collected UC samples and gain ethics committee approval to enroll this study at Tochigi Cancer Center Hospital, Utsunomiya Japan. GL and PAJ participated in the design, helped to perform statisitical analysis and collected UC samples and gain ethics committee approval to enroll this study at USC, LA, USA. KF and YH collected UC and healthy urine samples, and gain ethics committee approval to enroll this study at Nara medical university, Kashihara, Japan. HK participated in writing of the manuscript. All authors read and approved the final manuscript.

Acknowledgements
This work was supported in part by a Grant-in-Aid for Scientific Research 22791508 to YC from the Japan Society for the Promotion of Science, Japan.

Author details
[1]Department of Molecular Pathology, Nara Medical University, 840, Shijyo-cho, Kashihara, Japan. [2]Department of Urology, Nara Medical University, 840, Shijyo-cho, Kashihara, Japan. [3]Division of Molecular Pathology, National Cancer Center Research Institute, 5-1-1, Tsukiji Chuo-ku, Tokyo, Japan. [4]Department of Urology, National Cancer Center Hospital, 5-1-1, Tsukiji, Chuo-ku, Tokyo, Japan. [5]Oncogene Research Unit/Cancer Prevention Unit, Tochigi Cancer Center Research Institute, 4-9-13, Yonan, Utsunomiya, Japan. [6]Department of Urology, Tochigi Cancer Center Hospital, 4-9-13, Yonan, Utsunomiya, Japan. [7]Department of Urology, Norris Comprehensive Cancer Center, University of Southern California, 1441 Eastlake Ave, Los Angeles, CA, 90033, USA.

Received: 17 February 2013 Accepted: 22 May 2013
Published: 4 June 2013

References
1. Siegel R, Naishadham D, Jemal A: **Cancer statistics, 2013.** *CA Cancer J Clin* 2013, **63**:11–30.
2. Sugano K, Kakizoe T: **Genetic alterations in bladder cancer and their clinical applications in molecular tumor staging.** *Nat Clin Pract Urol* 2006, **3**:642–652.
3. Knowles MA: **What we could do now: molecular pathology of bladder cancer.** *Mol Pathol* 2001, **54**:215–221.
4. Van Rhijn BW, van der Poel HG, van der Kwast TH: **Urine markers for bladder cancer surveillance: a systematic review.** *Eur Urol* 2005, **47**:736–748.
5. Goessl C, Müller M, Straub B, Miller K: **DNA alterations in body fluids as molecular tumor markers for urological malignancies.** *Eur Urol* 2002, **41**:668–676.
6. Jones PA, Laird PW: **Cancer epigenetics comes of age.** *Nat Genet* 1999, **21**:163–167.
7. De Smet C, Loriot A, Boon T: **Promoter-dependent mechanism leading to selective hypomethylation within the 5' region of gene MAGE-A1 in tumor cells.** *Mol Cell Biol* 2004, **24**:4781–4790.
8. Yates DR, Rehman I, Meuth M, Cross SS, Hamdy FC, Catto JW: **Methylational urinalysis: a prospective study of bladder cancer patients and age stratified benign controls.** *Oncogene* 2006, **25**:1984–1988.
9. Dhawan D, Hamdy FC, Rehman I, Patterson J, Cross SS, Feeley KM, Stephenson Y, Meuth M, Catto JW: **Evidence for the early onset of aberrant promoter methylation in urothelial carcinoma.** *J Pathol* 2006, **209**:336–343.
10. Esteller M, Corn PG, Baylin SB, Herman JG: **A gene hypermethylation profile of human cancer.** *Cancer Res* 2001, **61**:3225–3229.
11. Yu J, Zhu T, Wang Z, Zhang H, Qian Z, Xu H, Gao B, Wang W, Gu L, Meng J, Wang J, Feng X, Li Y, Yao X, Zhu J: **A novel set of DNA methylation markers in urine sediments for sensitive/specific detection of bladder cancer.** *Clin Cancer Res* 2007, **13**:7296–7304.
12. Chan MW, Chan LW, Tang NL, Tong JH, Lo KW, Lee TL, Cheung HY, Wong WS, Chan PS, Lai FM, To KF: **Hypermethylation of multiple genes in tumor tissues and voided urine in urinary bladder cancer patients.** *Clin Cancer Res* 2002, **8**:464–470.
13. Friedrich MG, Weisenberger DJ, Cheng JC, Chandrasoma S, Siegmund KD, Gonzalgo ML, Toma MI, Huland H, Yoo C, Tsai YC, Nichols PW, Bochner BH, Jones PA, Liang G: **Detection of methylated apoptosis-associated genes in urine sediments of bladder cancer patients.** *Clin Cancer Res* 2004, **10**:7457–7465.
14. Hoque MO, Begum S, Topaloglu O, Chatterjee A, Rosenbaum E, Van Criekinge W, Westra WH, Schoenberg M, Zahurak M, Goodman SN, Sidransky D: **Quantitation of promoter methylation of multiple genes in urine DNA and bladder cancer detection.** *J Natl Cancer Inst 2006*, **98**:996–1004.
15. Vinci S, Giannarini G, Selli C, Kuncova J, Villari D, Valent F, Orlando C: **Quantitative methylation analysis of BCL2, hTERT, and DAPK promoters in urine sediment for the detection of non-muscle-invasive urothelial carcinoma of the bladder: A prospective, two-center validation study.** *Urol Oncol* 2011, **29**:150–156.
16. Nakajima T, Yamashita S, Maekita T, Niwa T, Nakazawa K, Ushijima T: **The presence of a methylation fingerprint of Helicobacter pylori infection in human gastric mucosae.** *Int J Cancer 2009*, **124**:905–910.
17. Wolff EM, Chihara Y, Pan F, Weisenberger DJ, Siegmund KD, Sugano K, Kawashima K, Laird PW, Jones PA, Liang G: **Unique DNA methylation patterns distinguish noninvasive and invasive urothelial cancers and establish an epigenetic field defect in premalignant tissue.** *Cancer Res* 2010, **70**:8169–8178.
18. Hemanek PS, Sobin LH: *UICC-International Union Against Cancer. TNM classification of malignant tumors.* 4th edition. Heidelberg, Germany: Springer-Verlag; 1987.
19. Chihara Y, Sugano K, Kobayashi A, Kanai Y, Yamamoto H, Nakazono M, Fujimoto H, Kakizoe T, Fujimoto K, Hirohashi S, Hirao Y: **Loss of blood group A antigen expression in bladder cancer caused by allelic loss and/or methylation of the ABO gene.** *Lab Invest* 2005, **85**:895–907.
20. Allred DC, Harvey JM, Berado M, Clark GM: **Prognostic and predictive factors in breast cancer by immunohistochemical analysis.** *Mod Pathol* 1998, **11**:155–168.
21. Negraes PD, Favaro FP, Camargo JL, Oliveira ML, Goldberg J, Rainho CA, Salvadori DM: **DNA methylation patterns in bladder cancer and washing cell sediments: a perspective for tumor recurrence detection.** *BMC Cancer* 2008, **8**:238.
22. Wolff EM, Liang G, Cortez CC, Tsai YC, Castelao JE, Cortessis VK, Tsao-Wei DD, Groshen S, Jones PA: **RUNX3 methylation reveals that bladder tumors are older in patients with a history of smoking.** *Cancer Res 2008*, **68**:6208–6214.
23. Christoph F, Weikert S, Kempkensteffen C, Krause H, Schostak M, Miller M, Schrader M: **Regularly methylated novel pro-apoptotic genes associated with recurrence in transitional cell carcinoma of the bladder.** *Int J Cancer* 2006, **119**:1396–1402.
24. Dudziec E, Gogol-Döring A, Cookson V, Chen W, Catto J: **Integrated epigenome profiling of repressive histone modifications, DNA methylation and gene expression in normal and malignant urothelial cells.** *PLos One* 2012, **7**:e32750.
25. Rauch TA, Zhong X, Wu X, Wang M, Kernstine KH, Wang Z, Riggs AD, Pfeifer GP: **High-resolution mapping of DNA hypermethylation and hypomethylation in lung cancer.** *Proc Natl Acad Sci USA* 2008, **105**:252–257.
26. Ehrlich M: **DNA hypomethylation in cancer cells.** *Epigenomics* 2009, **1**:239–259.
27. Pakneshan P, Tetu B, Rabbani SA: **Demethylation of urokinase promoter as a prognostic marker in patients with breast carcinoma.** *Clin Cancer Res* 2004, **10**:3035–3041.
28. Pulukuri SM, Estes N, Patel J, Rao JS: **Demethylation-linked activation of urokinase plasminogen activator is involved in progression of prostate cancer.** *Cancer Res* 2007, **67**:930–939.

doi:10.1186/1471-2407-13-275
Cite this article as: *Chihara et al.:* Diagnostic markers of urothelial cancer based on DNA methylation analysis. *BMC Cancer* 2013 **13**:275.

PLOS ONE

In Vivo Imaging of Enteric Neurogenesis in the Deep Tissue of Mouse Small Intestine

Kei Goto[1,2], Go Kato[3], Isao Kawahara[1,2], Yi Luo[2], Koji Obata[1], Hiromi Misawa[1], Tatsuya Ishikawa[3], Hiroki Kuniyasu[2], Junich Nabekura[3], Miyako Takaki[1,2]*

1 Department of Physiology II, Nara Medical University, School of Medicine, Kashihara, Nara, Japan, **2** Department of Molecular Pathology, Nara Medical University, School of Medicine, Kashihara, Nara, Japan, **3** Division of Homeostatic Development, Department of Developmental Physiology, National Institute for Physiological Sciences, Okazaki, Aichi, Japan

Abstract

One of the challenges of using imaging techniques as a tool to study cellular physiology has been the inability to resolve structures that are not located near the surface of the preparation. Nonlinear optical microscopy, in particular two photon-excited fluorescence microscopy (2PM), has overcome this limitation, providing deeper optical penetration (several hundred μm) in ex vivo and in vivo preparations. We have used this approach in the gut to achieve the first in vivo imaging of enteric neurons and nerve fibers in the mucosa, submucosa, submucosal and myenteric plexuses, and circular and longitudinal muscles of the small intestine in H-line: Thy1 promoter GFP mice. Moreover, we obtained clear three-dimensional imaging of enteric neurons that were newly generated after gut transection and reanastomosis. Neurogenesis was promoted by oral application of the 5-HT_4-receptor agonist, mosapride citrate (MOS). The number of newly generated neurons observed in mice treated with MOS for one week was 421±89 per 864,900 μm^2 (n = 5), which was significantly greater than that observed in preparations treated with MOS plus an antagonist (113±76 per 864,900 μm^2) or in 4 week vehicle controls (100±34 per 864,900 μm^2) (n = 4 both). Most neurons were located within 100 μm of the surface. These results confirm that activation of enteric neural 5-HT_4-receptor by MOS promotes formation of new enteric neurons. We conclude that in vivo 2PM imaging made it possible to perform high-resolution deep imaging of the living mouse whole gut and reveal formation of new enteric neurons promoted by 5-HT_4-receptor activation.

Citation: Goto K, Kato G, Kawahara I, Luo Y, Obata K, et al. (2013) In Vivo Imaging of Enteric Neurogenesis in the Deep Tissue of Mouse Small Intestine. PLoS ONE 8(1): e54814. doi:10.1371/journal.pone.0054814

Editor: Yvette Tache, University of California Los Angeles, United States of America

Received July 23, 2012; **Accepted** December 17, 2012; **Published** January 31, 2013

Funding: This study was supported by the Cooperative Study Program of National Institute for Physiological Sciences. This work was supported by Grants-in-aid for Scientific Research (20659210, 23390330, 24650325 for M.T. and 23591969 for H.M.) from the Ministry of Education, Science, Sports and Culture of Japan. The funders had no role in study design, data collection and analysis, decision to publish, or preparation of the manuscript.

Competing Interests: The authors have declared that no competing interests exist.

* E-mail: mtakaki@naramed-u.ac.jp

Introduction

Activation of enteric neural 5-HT_4-receptors by mosapride citrate (MOS) promotes the reconstruction of an enteric neural circuit injured after surgery, leading to the recovery of the 'defecation reflex' [1,2] in the distal gut of guinea pigs [3]. This neural plasticity involves neural stem cells [3]. Recently, we also revealed that MOS enhances neural network formation in gut-like organs differentiated from mouse embryonic stem cells [4]. Other 5-HT_4 receptor agonists also increase neuronal numbers and length of neurites in enteric neurons developing in vitro from immunoselected neural crest-derived precursors [5]. 5-HT_4 receptor-mediated neuroprotection and neurogenesis has also been demonstrated in the enteric nervous system of adult mice [6]. We therefore explored the ability of MOS to promote the generation of new enteric neurons at resected sites of the mouse small intestine *in vivo*. The new neurons are typically located in regions of granulation tissue, which is new connective tissue formed by growth of fibroblasts and blood capillaries into injured tissue after transection and reanastomosis of the gut.

Unfortunately, it is impossible for traditional fluorescence microscopy including confocal microscopy to perform high-resolution deep imaging of the 300–400 μm thick granulation tissue that is formed during the tissue repairing process at the anastomotic site after transection of the gut. Even in in vitro whole mount preparations, in which the mucosal, submucosal and circular muscle layers were removed, imaging of newly formed neurons and axons is severely limited. Nonlinear optical microscopy, in particular two photon-excited fluorescence microscopy, offers a means to overcome this limitation by providing enhanced optical penetration. Two-photon microscopy (2PM) allows cellular imaging several hundred microns deep in various organs of living animals and ex vivo specimens [7].

In the present study, we employed 2PM to obtain 3-dimensional reconstructions of impaired enteric neural circuits within the thick granulation tissue in the ileum of Thy1-GFP mice [8], in which the GFP is expressed in the cytoplasm of enteric neurons. Although in vivo imaging of the muscularis propria and myenteric neurons with probe-based confocal laser endomicroscopy in porcine models has been recently reported [9], we obtained the first ever (deleted) clear three-dimensional imaging of newly generated enteric neurons within the thick granulation tissue at the anastomosis, indicating that 2PM allows enteric neural imaging several hundred microns deep in the gut of the living mouse. The most critical challenge was to suppress movement artifacts to allow

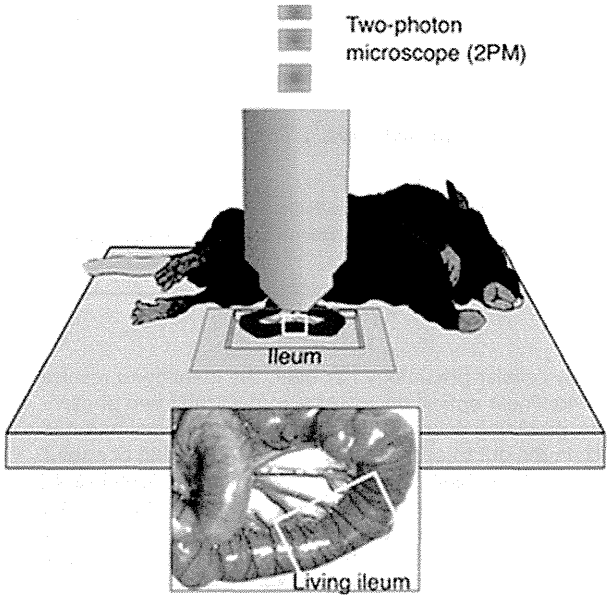

Figure 1. Depiction of the experimental approach for *in vivo* imaging of the intestine.
doi:10.1371/journal.pone.0054814.g001

for microscopy in the living gut. In addition, we tested whether activation of enteric neural 5-HT_4-receptors by MOS promotes reconstruction of an enteric neural circuit injured after the surgery as has been demonstrated in the lower gut [3].

Materials and Methods

Description and Preparation of Transgenic Mice Used for Imaging

All relevant experimental protocols were approved by the Ethics Review Committee for Animal Experimentation of the National Institutes for Physiological Sciences (permission number: 11A114). We used a transgenic mouse, based on the C57BL/6 strain, with sparse expression of cytoplasmic GFP in thalamic and cortical pyramidal neurons (Thy1 promoter GFP mouse, H-line) [8]. In preliminary studies, we confirmed expression of cytoplasmic GFP in enteric neurons. Transgenic mice, at 8–12 weeks after birth, were anesthetized with an intraperitoneal injection of Nembutal (50 mg kg^{-1}) and the abdomen was opened by a lower midline laparotomy. This approach spared vascular perfusion and maintained extrinsic inputs from the mesenteric nerves. The ileum was transected 5–6 cm from ileo-cecal sphincter and an end-to-end one-layer anastomosis was performed. Body temperature was maintained at 36–37°C using a heating pad. After recovery from the surgical procedure, mouse daily drank 0.1% DMSO vehicle solution (n = 5), MOS (100 μM) in vehicle (n = 6), or a selective 5-HT_4-blocker for oral application, SB-207266 (SB: 10–50 μM) [10] plus MOS (100 μM) in vehicle (n = 4) for 1 week (with the beginning two days fasting and the ending five days feeding ad libitum). In addition, vehicle controls were maintained for 4 weeks (n = 4) with the beginning two days fasting and the ending twenty-six days feeding.

In vivo Two-photon Microscopy

Seven days after the surgery, the mice were anesthetized with Nembutal (50 mg kg^{-1}) for in vivo microscopy. Body temperature was maintained at 36–37°C using a disposable pocket body warmer. Additional Nembutal was administered as needed. The depth of anesthesia was assessed by monitoring respiration rate and vibrissae movements. The abdomen was opened by a lower midline laparotomy and the surgical site of the ileum was fixed into the chamber for 2PM without disturbance of blood supply (**Figure 1**). To suppress ileal motility for microscopy, the preparation was pinned in place and papaverine (1 mM; 0.1–

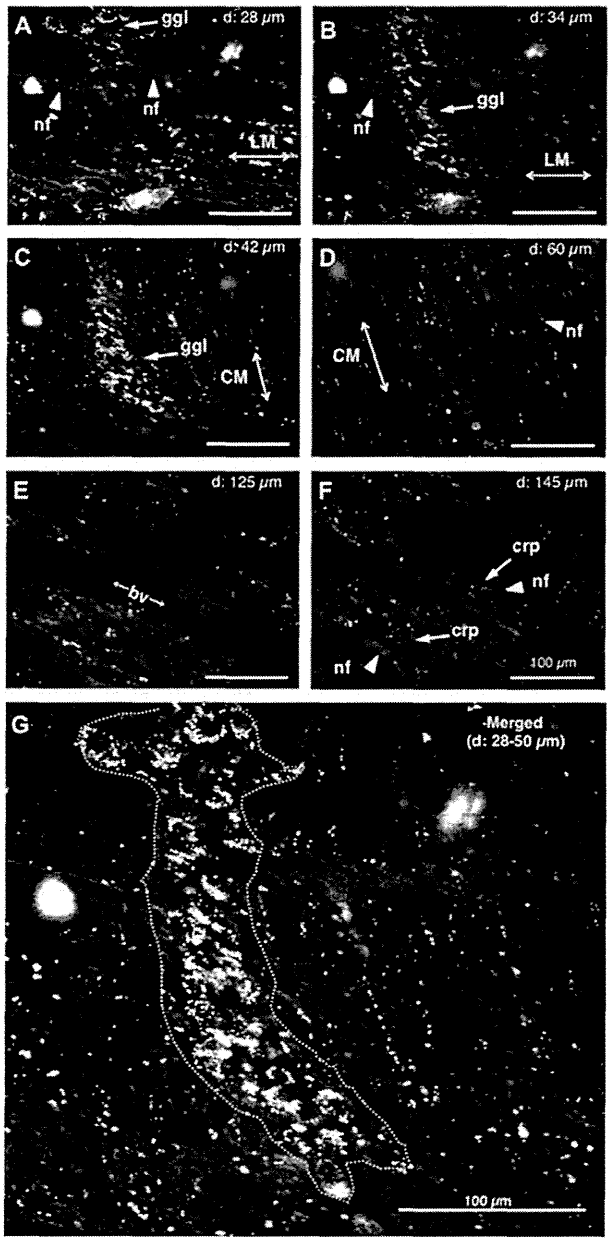

Figure 2. In vivo imaging of enteric neurons in the terminal ileum of an intact Thy1-GFP mouse. ***A.*** 28 μm deep to the serosal surface. ***B.*** 34 μm deep to the serosal surface. ***C.*** 42 μm deep to the serosal surface. ***D.*** 60 μm deep to the serosal surface. ***E.*** 125 μm deep to the serosal surface. ***F.*** 145 μm deep to the serosal surface. ***G.*** Merge of 28–50 μm deep images into a single image. Yellow arrows indicate ganglion (ggl) in ***A–C,*** and yellow arrowheads indicate nerve fibers in ***A, B, D*** and ***F,*** respectively. LM: longitudinal muscle. CM: circular muscle. bv: blood vessel. crp: crypt. Cal bar, 100 μm.
doi:10.1371/journal.pone.0054814.g002